FIFE Surface Climate and Site-Average Dataset 1987–89

ALAN K. BETTS AND JOHN H. BALL

Atmospheric Research, Pittsford, Vermont

(Manuscript received 14 May 1996, in final form 24 December 1996)

ABSTRACT

This paper analyzes the First ISLSCP (International Satellite Land Surface Climatology Project) Field Experiment site-average datasets for near-surface meteorology, soil moisture, and temperature; the surface fluxes of radiation, sensible, and latent heat; and the ground heat flux, for the period May 1987–November 1989. The diurnal and seasonal variation of surface albedo for this grassland site are discussed. The coupling of precipitation, soil moisture, evaporation, pressure height to the lifting condensation level, and equivalent potential temperature (θ_E) on seasonal and diurnal timescales is also discussed. The 1988 data confirm the authors' result, shown earlier from the 1987 data that over moist soils increased evapotranspiration lowers afternoon lifting condensation level and increases afternoon θ_E, suggesting a mechanism for a local positive feedback between soil moisture and precipitation on horizontal scales greater than 200 km. The seasonal cycle of ground heat flux and soil temperature is examined and the authors show that the coupling in the warm months between θ_E and soil temperature on seasonal scales is similar over land to the coupling found over warm oceans despite very different controls on the surface fluxes. The boundary layer equilibrium over the ocean is contrasted with the diurnal cycle over land, which is soil moisture dependent.

1. Introduction

The First ISLSCP (International Satellite Land Surface Climatology Project) Field Experiment (FIFE) was conducted on a 15 km × 15 km site centered at 39.05°N, 96.53°W near Manhattan, Kansas. The site is predominately grassland of moderate topography (Sellers et al. 1992). Surface data from ten Portable Automatic Meteorological (PAM) stations were collected from 1 May 1987 to 10 November 1989. During all three summers (1987, 1988, and 1989), surface flux measurements were made at many sites (22 sites in 1987, 10 in 1988, and 14 in 1989) (Kanemasu et al. 1992; Smith et al. 1992a,b; Nie et al. 1992; Fritschen and Qian 1992; Fritschen et al. 1992). The FIFE experiment has given insight into many aspects of the coupling between the surface and atmospheric boundary layer. Several papers have addressed the BL growth and BL-top entrainment issue (Betts 1992; Betts et al. 1992; Kelly 1992; Grossman 1992; Betts and Ball 1994; Betts and Barr 1996). Others have addressed the effect of surface heterogeneity (especially during the summer of 1989) on the surface fluxes (Desjardins et al. 1992), and secondary circulations produced by a soil moisture gradient (Smith et al. 1994).

This paper is a continuation of a study by Betts and Ball (1995), who analyzed the coupling of the diurnal cycle of the meteorological variables at 2 m during the 1987 season to the underlying land surface variables of soil moisture and soil temperature. They did this using a site-averaged time series of the measured surface fluxes, and meteorological variables from the PAM stations. This site-averaged time series also has been of great value in finding systematic errors in the formulation of the land–surface–atmosphere interaction in large-scale models (Betts et al. 1993; 1996a,b; 1997) and in the testing of new model parameterizations (e.g., Viterbo and Beljaars 1995; Chen et al. 1996; and others). Our initial mean time series extended only from May to October 1987, and there is considerable interest by projects such as the Pilot Intercomparison of Land-Surface Parameterization Schemes (PILPS) for time series that extend more than 12 months. Accordingly, we have generated for further model studies a site-average time series of the PAM data for the entire FIFE experiment as well as site surface flux and soil moisture averages for the three summer time periods. Since the three years were different meteorologically (in particular, the spring and early summer of 1988 was a period of drought over the central United States), this paper intercompares the three years to see whether the conclusions reached in Betts and Ball (1995) are applicable to the following years for the same site. We also extend our analysis of the coupling of equivalent potential temperature (θ_E) to soil temperature, and of soil moisture to the pressure height to the lifting condensation level pressure (P_{LCL}), defined as

Corresponding author address: Dr. Alan K. Betts, R.D. #3, Box 3125, Pittsford, VT 05763
E-mail: akbetts@aol.com

$$P_{\mathrm{LCL}} = p_s - p^*, \quad (1)$$

where p_s is the surface pressure, and p^* is the saturation pressure of surface air (Betts and Ball 1995).

The model purist may argue that the land surface interaction is too nonlinear to permit averaging over a diverse set of sites. However, at the individual site level the data quality and data sampling problems are so severe that the seasonal hydrology on a site basis makes little physical sense (see Duan et al. 1996). By averaging upscale, we can get an almost continuous time series for most variables in which plausible physical connections between, say, soil moisture and site-average evaporation are readily visible. There is still much to be done to properly represent the land surface interaction in large-scale models averaged over the scale 10–50 km, and we believe this site-average dataset can give valuable guidance for this.

As models for the land surface increase in complexity in their representation of the vegetation and subsurface hydrology, it is easy to lose sight of fundamental thermodynamic links in the detail. One aim of this paper is to contrast the land and ocean surface boundary conditions. Over the oceans, the daytime solar heating is absorbed in a deep ocean mixed layer, and the diurnal cycle of surface temperature is small (except at very low wind speeds). The sun's energy warms the ocean mixed layer on seasonal timescales. Since the surface is saturated, evaporation is the dominant surface heat transfer, and this is primarily controlled by the surface wind and the large-scale subsidence of dry air from above (see, e.g., Betts and Ridgway 1989). The solar heating and surface evaporation are not coupled on short timescales (as over land), but only on the seasonal timescale through the sea surface temperature. In contrast, over land the solar heating drives a strong diurnal cycle in both air and near-surface soil temperature, and only a small fraction of the surface net radiation is stored in the soil, driving the seasonal cycle of soil temperature. On the daily timescale, the surface fluxes are coupled to the net radiation. On weekly and seasonal timescales, the mean air 2-m temperature and 10-cm soil temperature are, however, closely coupled just as over the ocean (for the FIFE grassland, but not over the boreal forest, where there may be a thick moss layer; Betts et al. 1996a). Consequently on weekly to seasonal timescales, the daily average 2-m θ_E and the 10-cm soil temperature are also closely coupled, as they are over the oceans. The large diurnal variation is imposed on top of this seasonal trend. The other key difference between vegetated land and ocean surface boundary conditions is that (except when the land surface is wet following recent precipitation), evapotranspiration is dominated by transpiration, which is stomatally controlled. The air over the surface of transpiring leaves is not saturated so that the balance of saturation pressure (see Betts 1992, 1994) over land is fundamentally different than over the ocean. There we see saturation at the surface, whereas over vegetation the saturation pressure deficit increases with decreasing soil moisture (and increasing stomatal resistance). As a result, when the diurnal boundary layer (BL) evolution is considered, we find a strong link between soil moisture and the diurnal rise of P_{LCL} (the surface saturation pressure deficit or the pressure height of the lifting condensation level). Over the ocean P_{LCL} is usually also the height of cloud base and varies rather little. This paper addresses these links between soil temperature and soil hydrology, and the seasonal and diurnal cycle using the FIFE data from 1987 to 1989.

2. Data processing

The appendix summarizes the site-average datasets that are now available from the authors. Users of the data are reminded that 1988 was a leap year.

a. PAM mesonet data

The biggest difficulty in generating an interannual meteorological and radiation flux time series, averaged over the FIFE site, was cleaning up the data. The Portable Automated Meteorological stations are interrogated by satellite and the archive time series of 30-min averages (themselves generated from 5-min averages) from each station contain spurious and missing data. The instrument electronics were also affected by summer storms. Our approach was a simple one (Betts et al. 1993, appendix). To each time series we applied range filters to exclude physically unrealistic data; we then intercompared the time series at all ten PAM stations with the mean and standard deviation to look for erroneous data from single stations. We did extensive manual editing of the individual time series, before generating a final mean, count, and standard deviation of the remaining data. We made no attempt to fill in gaps in individual time series before averaging, so that the mean does fluctuate if a single site (e.g., with more extreme properties, a wet valley, or rocky hillside) drops in and out of the time series. We made no attempt to account for land cover in the average, although the PAM sites had been selected to be in some sense representative of the terrain. The critical humidity measurement was made by wet-bulb and dry-bulb thermistors (respectively T_w and T); so we looked carefully for indications of dry wet-bulb wicks and deleted this data. We calculated a mixing ratio for each good (T, T_w) pair and used these to derive the site average. Humidity is unknown in winter whenever it is cold enough to freeze the wet-bulb instrument. The PAM dataset we have prepared includes the standard meteorological variables, rainfall, two soil temperatures (at 10 and 50 cm) and net radiation, the incoming and reflected solar radiation, longwave flux down, and a radiometric skin temperature.

b. Surface flux data

The second dataset we have generated is a site-average ''FLUX'' time series from the measurements collected by many individual principal investigators. The number, distribution, and duration of these sites varies from summer to summer. No surface flux measurements (other than radiation from the PAM stations) were made outside the April–October time period. In 1987, the main focus was on four short Intensive Field Campaigns (IFCs), when there were as many as 22 surface flux stations (6 sites measuring fluxes by the eddy correlation method and 16 by the Bowen ratio method). The time periods of these four IFCs in 1987 were 26 May–6 June, 25 June–11 July, 6–21 August, and 5–16 October. In 1987 6 Bowen ratio sites were fully operated all summer, and 2 others made enough measurements to reconstruct a continuous time series of sensible and latent heat. In 1988, 6 Bowen ratio sites operated for most of the summer (10 May–16 Sep), and at times as many as 10 were operating. In 1989 flux measurements only exist for a short IFC-5 from 24 July to 12 August from 14 sites.

c. Soil moisture data

Soil moisture was systematically measured at a large number of sites by two methods: one gravimetric for the near-surface layer 0–10 cm and a second using neutron probes to depths of up to 2 m (the neutron probe measures volumetric soil moisture). In 1987 there were 20 gravimetric sites (each of which typically made measurements at five locations) and 31 neutron probe sites. Measurements were made at near-daily intervals during IFCs and less frequently between them. In 1988 21 sites took gravimetric measurements and 11 took neutron probe measurements, typically every 5–7 days, and in 1989, during the short IFC, there were daily gravimetric and less frequent neutron probe measurements at 13 sites. Each vertical profile of neutron probe measurements was merged in the FIFE archive with a proximate subset of the gravimetric measurements for the layer 0–10 cm, converted to volumetric soil moisture by multiplying by a bulk density.

To generate a FIFE site average, we first averaged measurements at each site, then interpolated to get a value for each site for every day, and then averaged these values to get a daily FIFE site average. Interpolation was necessary, before generating a FIFE site average, because not every site was measured on any given day, especially in 1988 when sampling was less frequent. For users of this dataset we provide a count of the total number of actual observations that were made (regardless of location) on a given day, which gives some indication of the days for which soil moisture is smoothed (and permits some adjustment for days immediately preceding major rain events). In this paper, we shall frequently stratify data based on the site average of the full set of measurements of 0–10-cm soil moisture. These measurements were made gravimetrically, and we have converted them to a volumetric soil moisture by multiplying by a bulk soil density of 1.1. In our previous papers (Betts et al. 1993; Betts and Ball 1995), we incorrectly interpreted the FIFE bulk soil density measurements in converting gravimetric to volumetric soil moisture so that the volumetric values in those papers are low (see appendix 1c).

3. Seasonal comparison of the summers of 1987, 1988, and 1989

The information contained in 2½ years of data is huge, so we will focus in this paper on a few key energetic aspects of the land surface–atmosphere interaction. The first is the relationship between rainfall, soil moisture, vegetation, surface evaporation, and the diurnal cycle of cloud base and θ_E in midsummer, which was one focus of our previous paper (Betts and Ball 1995). The second is the seasonal and diurnal cycle of the surface radiation budget and albedo. The third is the seasonal cycle of soil temperature and its links to the equivalent potential temperature, θ_E, at 2 m, which has received rather little attention previously.

a. Rainfall, surface hydrology, vegetation, and evaporation

Figures 1a–c compare the monthly precipitation (P in mm) for the three years, and the hydrologic budget terms, evaporation (E) and soil moisture (SM), change in the first 2-m depth for the summer months in 1987 and 1988 for which we have complete data.

The PAM stations started operating 1 May 1987, and we have added monthly precipitation for January–April 1987 (and December 1989) from the daily precipitation records of the Long Term Ecological Research Center, which is a subarea in the northwest of the FIFE site. In 1987 (Fig. 1a) July was the driest month: there was no rainfall from 19 July to 2 August. From the FLUX data and neutron probe soil moisture data, we have calculated the corresponding site-average monthly evaporation (E in mm) and integrated SM change (in mm) for a nominal 2-m soil depth for the four months June–September for which we have a complete time series. In June and July 1987, evaporation exceeded precipitation, and the corresponding drop of column soil moisture is visible. In August, heavy rainfall exceeded evaporation, and the soil moisture was partly replenished, only to fall again in September.

This hydrological balance is not exact. Over the full summer period 29 May–16 October 1987 for which we have complete data, the site-averaged ($P - E$) is -146 mm, whereas the measured change of soil column moisture is -107 mm; a difference of 40 mm. In one earlier study, Viterbo and Beljaars (1995) found a larger water imbalance of 100 mm, using our earlier datasets. We have reduced this by carefully reexamining the precip-

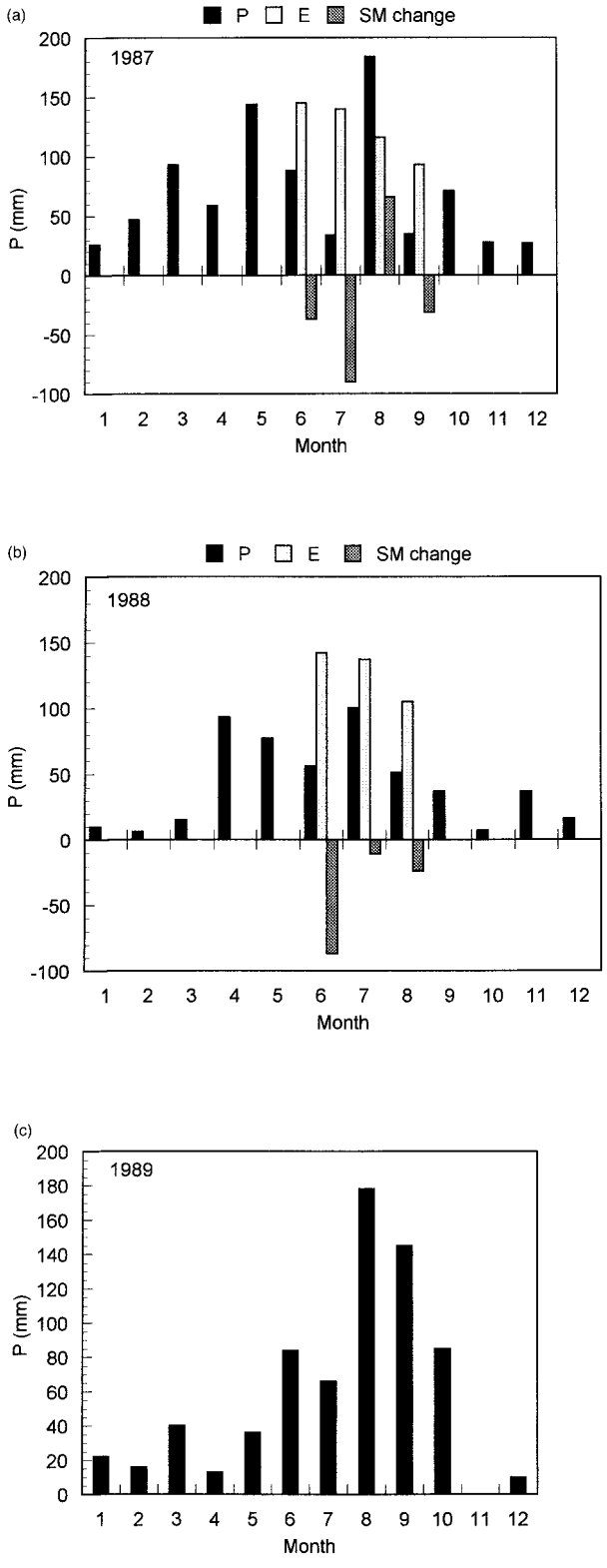

FIG. 1. Monthly precipitation (mm) for the FIFE site for 1987. Monthly evaporation (mm) and change of soil moisture (mm) in first 2-m depth are shown for June–September. (b) As in (a) but for 1988 with evaporation and soil moisture change for June–August. (c) As in (a) but for 1989 precipitation only.

itation time series from the PAM stations, which has increased the total precipitation; in addition our new FLUX time series, which includes more stations, has less total evaporation. Another study (Duan et al. 1996) found a smaller water imbalance of only 20 mm, but their precipitation estimates are higher than ours. Runoff was measured only in 1987 for a small catchment (Famiglietti et al. 1992) representing only 10% of the FIFE area. For the summer 1987 budget time interval, the total runoff for this catchment was only 27 mm (Duan et al. 1996), and it may not be representative of the whole FIFE area, so we have neglected runoff. We include this discussion because the long-term hydrological balance at the surface is so difficult to model satisfactorily (Viterbo and Beljaars 1995). Yet accurate measurement of basic variables such as precipitation, evaporation, and soil moisture is also very difficult. For example, we used a nominal soil depth of 2 m since we have neutron probe measurements at some sites to this depth, although the median soil depth is only 1.5 m (Duan et al. 1996). The 1987 neutron probe data at 20 cm is questionable (see appendix 1c), but excluding it only alters the seasonal soil moisture budget by 1 mm. While the FIFE datasets give considerable insight into interactions at the surface, they have limitations for long-term hydrological studies.

Figure 1b shows the monthly precipitation for 1988 and the monthly evaporation and column soil moisture change for June, July, and August. The spring and early summer was drier than 1987, and indeed there was a drought across much of the central United States. June was, in fact, much drier than the monthly total suggests, as the drought was broken with 30 mm of rain on 30 June. For the whole period 10 May–19 September 1988 for which we have flux data, $P - E = -213$ mm, while column soil moisture falls only 100 mm: a much larger imbalance than in 1987. We have no explanation for this and repeat our caution above.

Figure 1c shows just the precipitation in 1989, which was very dry in spring, and only had sufficient rainfall to match evaporation in August and September. There is however no complete month of FLUX data or soil moisture data. Rainfall was also rather heterogeneous across the FIFE site in the summer of 1989 (Smith et al. 1994).

Figure 2a summarizes the interaction between the rainfall, soil hydrology, vegetation, and summer evaporation for 1987. The lowest curve (dotted, with scale on right) shows the episodic daily precipitation in millimeters. The light solid curve (scale on left) is the site-average 0–10-cm volumetric soil moisture (calculated from gravimetric samples). During the four IFCs, samples were collected almost daily; otherwise less frequently. The drop of soil moisture during the periods of little rainfall (Julian day 150–163, 200–213, and 262–282) is clearly visible. The lowest soil moisture is reached at the beginning of August, after 2 weeks of no rain. The dashed curve (scale on left) shows mean ''af-

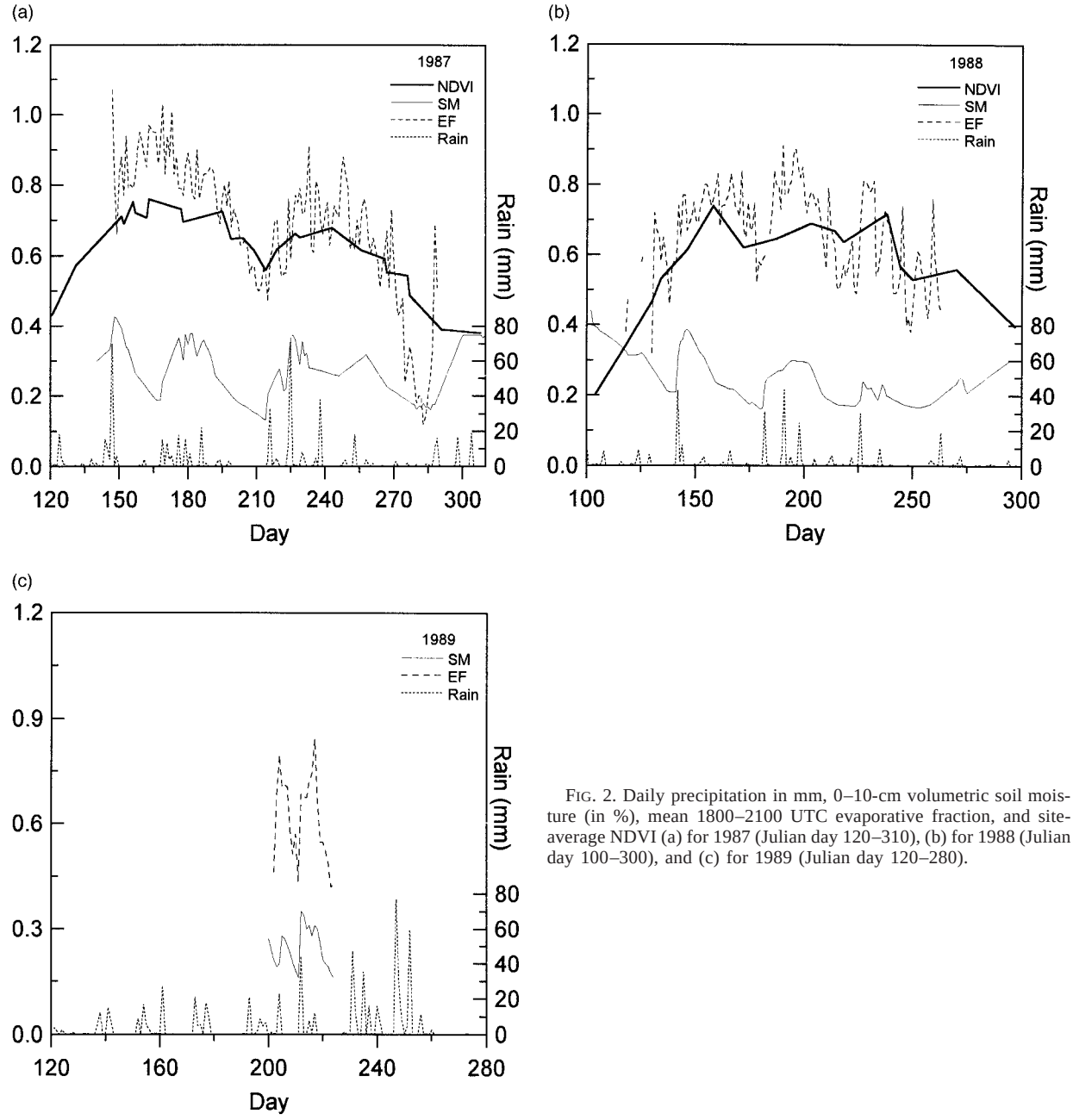

FIG. 2. Daily precipitation in mm, 0–10-cm volumetric soil moisture (in %), mean 1800–2100 UTC evaporative fraction, and site-average NDVI (a) for 1987 (Julian day 120–310), (b) for 1988 (Julian day 100–300), and (c) for 1989 (Julian day 120–280).

ternoon'' evaporative fraction, EF (a site average from 1800 to 2100 UTC; local noon being 1820 UTC). We define EF as

$$\mathrm{EF} = \overline{\mathrm{LH}}/(\overline{\mathrm{SH}} + \overline{\mathrm{LH}}), \qquad (2)$$

where $\overline{\mathrm{SH}}$ and $\overline{\mathrm{LH}}$ are surface sensible and latent heat respectively, averaged for the 1800–2100 UTC period.

The fall of EF during the late July dry-down is very apparent. Some fall of EF can be seen in the second half of September as the soil dries, but the large fall of EF around 1 October (day 274) is with the first killing frost. In contrast in June, although 0–10-cm soil moisture falls, no drop of EF is visible. We are unsure whether the EF data is unreliable during this between-IFC period early in the experiment or whether at deeper levels the soil is still sufficiently wet this spring (the 20-cm neutron probe data is questionable in 1987). The heavy solid curve shows a site average of the normalized difference vegetation index (NDVI), derived from polar orbiting satellite observations (Advanced Very High Resolution Radiometer) by Hall et al. (1994). This shows the seasonal cycle of vegetation. Note that NDVI also follows soil moisture during the late July period.

Figure 2b shows the corresponding plots for 1988 for

the time period of surface flux and soil moisture measurements. The pattern of rain in 1988 is different. There was a dry spring (and a drought across the central United States). The sampling of soil moisture is less frequent than in 1987. Three dry-downs in the 0–10-cm soil moisture are visible in May (130–140), June (150–180), and early August (210–224). The dashed curve shows the drop of EF associated with these drops of soil moisture, together with the day to day fluctuations of EF, that are largely associated with advection and each individual rainfall event.

Figure 2c shows the summer of 1989, for which there is only a brief 20-day period when soil moisture and surface flux data are available. Spring of 1989 was again dry (Fig. 1c). Conditions across the FIFE site were much more inhomogeneous in 1989 than 1987, but even in this site average, the link between soil moisture and daytime EF is clearly visible.

The observational picture given by Figs. 2a–c is encouraging as it shows clearly that the link between soil hydrology and evaporation, which has been reported for individual sites (Sellers et al. 1992; Stewart and Verma 1992; Verma et al. 1992; Smith et al. 1992b), still holds for these FIFE averages. The figures also show that the variation of NDVI has links to soil moisture, as well as the seasonal cycle. However, that EF does not fall in June 1987 (150–163), during the period of peak spring green-up when 0–10-cm soil moisture falls but moisture is probably available at deeper levels, suggests that modeling the link between vegetative resistance and soil moisture at different levels is not simple. However, we are unsure whether the EF data are reliable (or representative) for this early period (when only a few sites are running between the IFCs).

b. Radiation budget

Accuracy in the surface radiation budget plays a key role in the land-surface boundary condition in forecast models. Atmospheric absorption of the increasing solar radiation is important, and also reflection and absorption by clouds. At the surface the albedo plays a key role in the surface energy budget.

1) SOLAR RADIATION

Figure 3 shows the daily averaged incoming solar radiation against Julian day for the three years. The upper envelope represents clear sky values, ranging from a daily mean of 350 W m^{-2} in midsummer to a little over 100 W m^{-2} in midwinter. Note that on rainy and cloudy days, $S\downarrow$ falls by about 60% typically. The large gap from 11 April to 11 May 1988 was the time when all the radiometers were removed for calibration. The solar radiation peaks are a little higher in 1987 than 1988, but the sampling is poorer in 1988. The sampling strategy for the PAM stations was to measure the reflected solar radiation at all sites (to account for the heterogeneity of the surface), but to measure incoming solar at only a few sites. Unfortunately in 1988, which was not a year of intensive field campaigns, this often meant that only one or two incoming solar instruments on the PAM stations were operating, and the sampling is correspondingly poor. In 1989 there were usually four instruments working. During the summer of 1988, however, there were in addition six flux sites measuring incoming and reflected solar radiation (not shown).

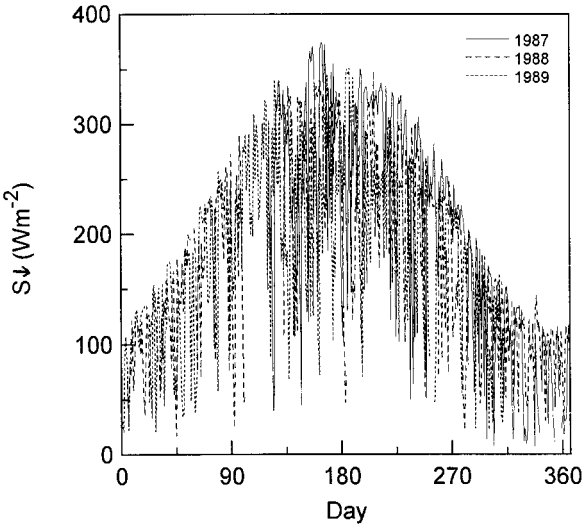

FIG. 3. Daily average incoming solar radiation for the three years (1 May 1987–10 November 1989).

The corresponding envelope of the daily average net radiation, R_n, (not shown) for the three years looks very similar to Fig. 3. The range is from 25 W m^{-2} in midwinter to 200 W m^{-2} in midsummer.

2) SEASONAL VARIATION OF ALBEDO

In numerical models the surface albedo plays a key role in the surface energy budget. We first calculated daily average albedo (calculated by first averaging separately $S\downarrow$ and $S\uparrow$ for each day from the PAM data) for the three years for all days where there is significant daytime data. The daily average in summer is near 0.18 (not shown). There are spikes of albedo in winter after snowfall (not shown), when albedo typically rises to 0.6–0.8; but albedo rarely stays high over this location in Kansas for more than a few days (because the temperature usually rises above freezing). In winter when the albedo is high because of snow, the diurnally averaged net radiation is near zero (not shown). Figure 4 shows the albedo calculated from all the data from the three years, in 30-day bins (absorbing 2 or 3 extra days at the beginning and end of the year into the first and last bins. The mean seasonal cycle of ''climatic'' albedo is now visible: there is relatively little variation from April to September from an average daily value of 0.18

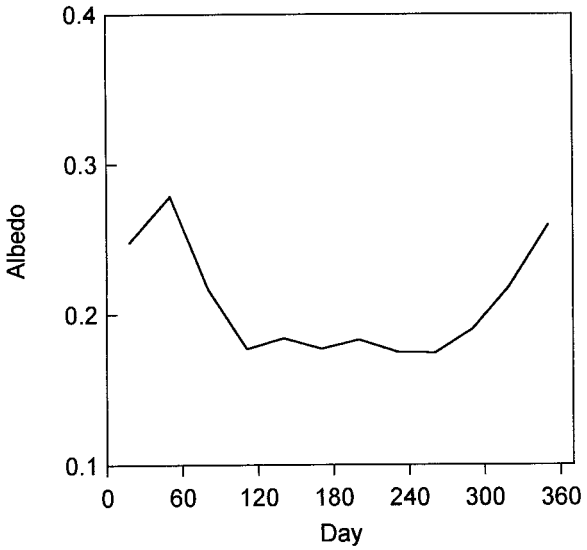

FIG. 4. FIFE site 30-day averaged albedo for 1987–89.

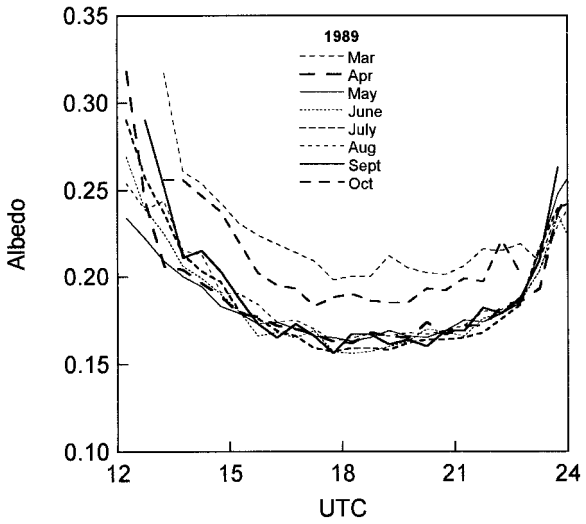

FIG. 5. Daytime albedo for March–October 1989. (Local solar noon is 1820 UTC.)

for this grassland site, with an increase due to episodic snowfall in the winter months to about 0.25.

3) DIURNAL VARIATION OF ALBEDO

Figure 5 shows the diurnal variation of albedo for 1989 for March–October. The lowest monthly mean albedo at noon from May to September are similar (~0.16), with sharp rises toward sunset, as the solar zenith angle increases. October has a higher albedo after the senescence of the vegetation. March is higher still because it includes a few snow-covered days.

The diurnal variation with solar zenith angle is important to the surface energy balance, particularly in the evening, when the rise of albedo causes the surface temperature to fall more rapidly from its afternoon peak, than if the albedo were constant. As a result the surface uncouples sooner from the BL; as soon as the surface (virtual) sensible heat flux goes negative. Not representing the diurnal variation of albedo can produce errors in models. Figure 6 shows the error in the shortwave surface energy balance, if a fixed midday value of albedo is used. The two curves are averages from May to August for 1987 and 1989 of

$$\Delta \mathrm{SW} = \alpha_{\mathrm{noon}} S\downarrow - S\uparrow. \qquad (3)$$

The PAM sensors were moved between the two years and the asymmetries between the years probably reflect only small errors in instrument alignment. The rise of albedo toward sunset reduces the net shortwave flux by ~12 W m^{-2}, which in turn may reduce the radiative equilibrium skin temperature by about 2 K. This accelerates the uncoupling of the surface from the BL in the early evening.

c. Soil temperature

Figure 7 shows the annual cycle of daily averaged air temperature T, and soil temperatures T_{soil10} and T_{soil50} at 10 cm and 50 cm depth for 1988, the only year with a complete record. The lag of the soil temperatures behind the rapidly fluctuating air temperature can be seen. Note that the soil at 50 cm does not freeze in winter. Figure 8 intercompares the 10-cm soil temperatures for the three years. Although the seasonal cycles are similar, there are some significant differences between the years. At 10-cm, 1989 is generally cold all summer. In May (day 121–151) 1988 is cooler than 1987, and 1989 is even colder. In September (244–273) 1989 is cooler. Although these differences may seem small, soil tem-

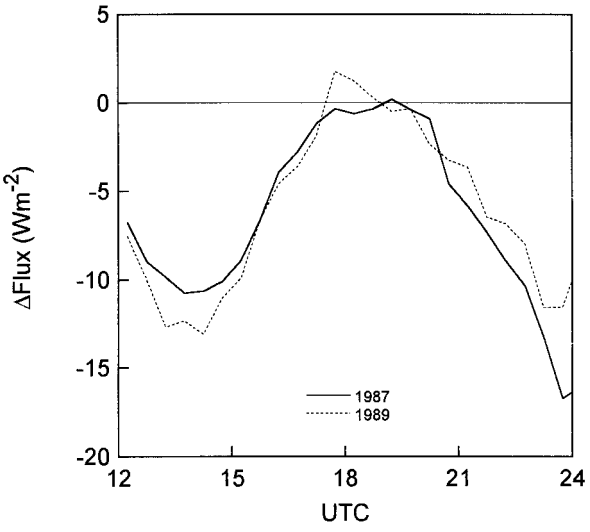

FIG. 6. Surface flux error from assuming fixed noon value of albedo (see text).

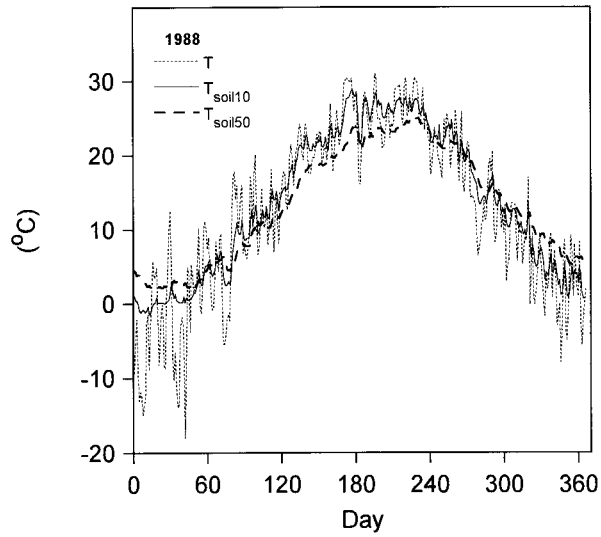

FIG. 7. Annual cycle of daily averaged 2-m air temperature and 10-cm and 50-cm soil temperatures for 1988.

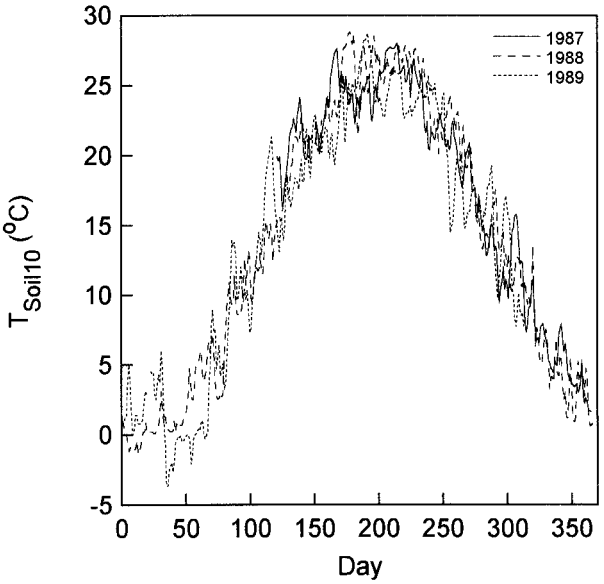

FIG. 8. 10-cm soil temperature for 1987–89.

perature has a strong coupling to the 2-m equivalent potential temperature (θ_E), so we will see later the impact of these different soil temperatures on the monthly mean diurnal cycle at 2 m.

d. Ground heat flux and net radiation

The fraction of net radiation conducted as a heat flux into the soil determines the daily and seasonal cycles of soil temperature. The seasonal cycle depends on the daily average soil heat flux, while the diurnal amplitude depends on the daytime soil heat flux. The difference between net radiation and ground heat flux is the surface condition driving the diurnal cycle of θ_E over land (Betts 1992; Betts and Ball 1995; Eltahir 1996).

1) SEASONAL DIURNAL PATTERN

Figure 9 shows for 1988 the diurnal pattern of the measured ground heat flux, G, and net radiation, R_n, stratified by month. (The months May and September are incomplete since this FLUX time series runs from 10 May to 19 September 1988.) The diurnal cycle of R_n shows a daytime peak in May and June, partly because of the solar cycle but also because these months were drier and had probably less mean cloudiness than say July. The ground heat flux G shows a clear seasonal cycle. The diurnal amplitude is largest in May, as the soil warms in the spring. By September, the amplitude is small and the daily average G is slightly upward. In spring, the diurnal amplitude of soil temperature is also greater (not shown), as expected from the larger amplitude of G. In 1987 (not shown) the pattern is similar, although G is somewhat larger in all seasons; probably because the sampling of FLUX sites is different.

2) RATIO G/R_n AND ITS DEPENDENCE ON SOIL MOISTURE

Figure 10a shows the ratio G/R_n from 1988, stratified by month. The peak daytime ratio falls from 0.15 in May to 0.08 in September, but the ratio shows no clear seasonal pattern at night (July is above May and June). In 1987 (not shown) the peak daytime ratio is higher: 0.18 in June.

Dry soils have a lower thermal conductivity than wet soils, so there is a possible link between soil moisture and ground heat flux. Figure 10b shows the diurnal variation of the ratio G/R_n for 1988, stratified by volumetric soil moisture in the first 10 cm. (This stratification is

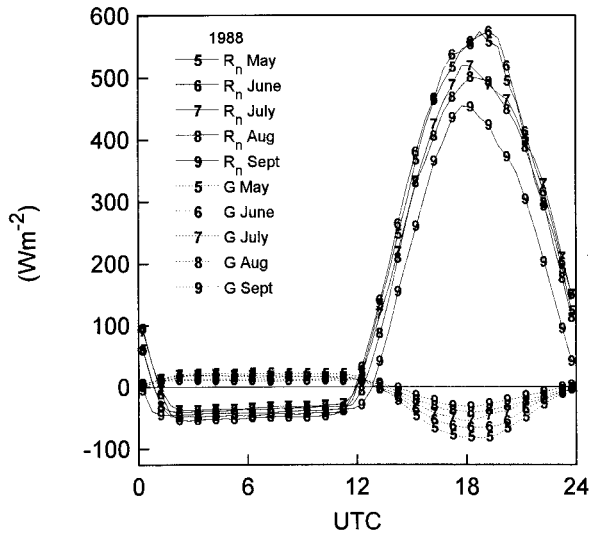

FIG. 9. Diurnal curves of monthly R_n, G for 1988 FLUX data. (May and September are incomplete months.)

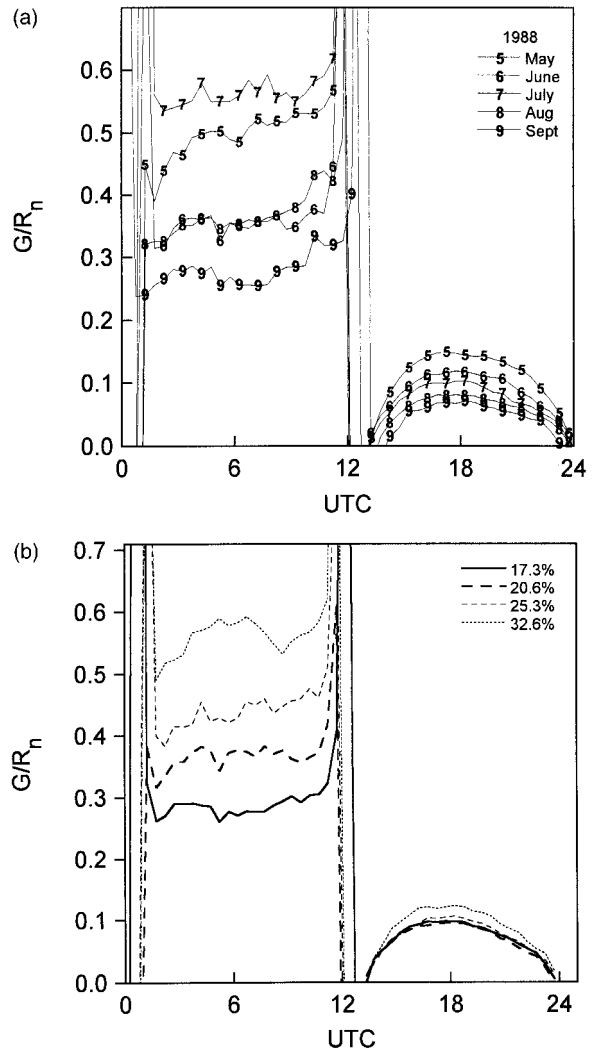

FIG. 10. As in Fig. 9 but for the ratio G/R_n, stratified by month and (b) stratified by 0–10-cm soil moisture ranges shown in Table 1.

discussed more fully later, together with Table 1.) The apparent small decrease in the daytime ratio with soil moisture may only reflect the seasonal trend since the drier averages have a later average date than the wet averages. However, unlike Fig. 10a, there is a clear pattern at night: the upward ground heat flux is much less when the soil is dry. In 1987 (not shown) the pattern at night is similar, when we stratified by soil moisture, although no daytime pattern was evident.

e. Seasonal diurnal cycle

The impact of the surface fluxes on the atmosphere, particularly moist convection, is controlled by the diurnal variation of the boundary layer temperature and humidity. As in Betts and Ball (1995), we shall assume that the variations of the 2-m variables are representative of the variation of BL variables. Betts and Ball (1995) showed the seasonal cycle of the diurnal cycle at 2 m by plotting hourly values of potential temperature, θ, against mixing ratio, q (their Fig. 10). Here we carry this representation further by plotting the pressure height of the lifting condensation level, $P_{\rm LCL}$ (which is a measure here of how far surface air is from saturation), against equivalent potential temperature, θ_E (which defines the temperature path of air ascending in clouds). Either coordinate system can be derived from the other, but the advantage of ($P_{\rm LCL}$, θ_E) is their more direct role in *linking near-surface parameters to atmospheric moist convection.* On seasonal timescales, daily mean θ_E is linked to the mean soil temperature (see section 4a), and the rise of θ_E to its afternoon maximum is linked to the available energy ($R_n - G$, a θ_E source: see Betts and Ball 1995), and the downward entrainment of low θ_E air at the BL top. In midsummer, when soil temperatures are warm and vary little, the dependence of θ_E on soil moisture is visible [Betts and Ball (1995) and section 5]. In turn, instability for moist convection depends on BL θ_E. The variable $P_{\rm LCL}$ is linked to the availability of water for evaporation, either from the soil moisture through evapotranspiration or direct evaporation from the soil if wet, and the imbalance between these surface sources, and the mixing down of highly unsaturated air into the BL from the free atmosphere (Betts 1992, 1994; Betts and Ball 1995). On rainy days, the evaporation of falling precipitation can also reduce $P_{\rm LCL}$ directly as it brings air closer to saturation, although intense organized convection can bring down dry air of high $P_{\rm LCL}$ into the BL in unsaturated downdrafts. In turn, $P_{\rm LCL}$ is an indicator of the height of cloud base (although over Kansas in summer, the cloud base may be higher than

TABLE 1. Stratification by volumetric soil moisture (SM).

Year	SM range (%)	$\overline{\rm SM}$ (%)	Number of days	R_n (W m^{-2})	G (W m^{-2})	EF	$P_{\rm LCL}$ (mb)	V_s (m s^{-1})	$\Delta T_{\rm rad}$ (K)
	<18.5	16.0	15	570	90	0.59	214	4.6	6.3
	18.5–23	20.2	16	547	68	0.70	172	3.0	3.7
	23–29	25.9	33	535	66	0.73	156	2.1	2.8
1987	>29	33.5	29	554	81	0.77	127	1.6	2.5
	<18.5	17.3	24	530	47	0.54	197	3.2	7.1
	18.5–23	20.6	25	553	47	0.67	192	3.6	5.9
	23–29	25.3	17	588	55	0.76	154	2.6	5.3
1988	>29	32.6	16	584	66	0.77	134	3.8	3.7

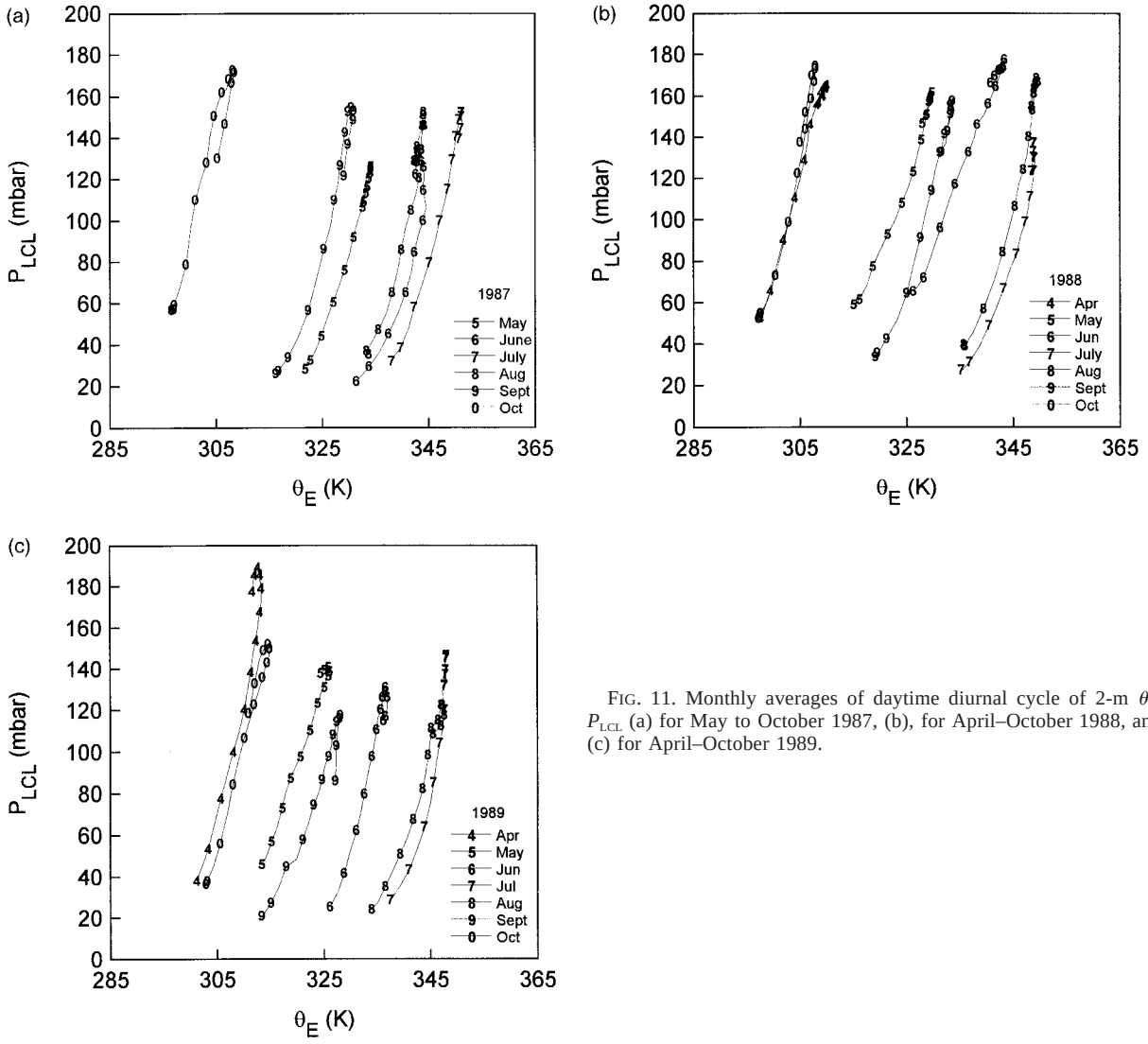

FIG. 11. Monthly averages of daytime diurnal cycle of 2-m θ_E, P_{LCL} (a) for May to October 1987, (b), for April–October 1988, and (c) for April–October 1989.

the LCL of surface air); which together with θ_E is an important control on deep convection and precipitation. Because soil moisture is not replenished over land unless it rains (unlike the ocean), these feedbacks between surface processes and atmospheric convection have a particular role over land.

Figures 11a–c show the daytime monthly mean diurnal cycles from 1115 to 2315 UTC for the months April (May in 1987) to October for the three years 1987–89. For each month, the lowest point represents the atmospheric state shortly after sunrise, when the air is cool and close to saturation (which would be $P_{LCL} = 0$). The points are hourly from 1115 UTC showing the daily rise of θ_E and P_{LCL} to an afternoon maximum and then its subsequent fall. For each year, the July curves are on the right, as this is the month when θ_E (and soil temperature) are highest, but the sequence of months is not the same in every year. For example, the month pairs 5 and 9, 6 and 8 are reversed in 1987 and 1988. On average the soil temperature was cooler in May and warmer in September in 1988 than in the corresponding months in 1987 (see Fig. 8). In addition the afternoon mean maximum of P_{LCL} is very different in the same month in different years. Not surprisingly, the months with high P_{LCL} (April 1989 and June 1988: recall that 30 mm of the June 1988 rainfall in Fig. 1b fell on 30 June) were months of little rainfall. Months of low mean P_{LCL} (May 1987 and August 1989) had high rainfall. Qualitatively the monthly mean diurnal cycle is linked both to soil moisture (through rainfall) and to soil temperature (although the seasonal cycle of soil moisture can be large, and in some months advection may also be important). We will explore these links further in the next sections. Exceptions can be seen on the monthly timescale. August 1987 and 1989 had similar rainfall, but P_{LCL} in 1987 would suggest a ''drier'' month. The

reason may be that much of the rainfall in August 1987 (>80 mm) fell on 12–13 August after nearly a month of drought. An August 1987 average combines extremely dry conditions at the beginning of the month with moister soils for the later half, whereas in August 1989 the period without rain was much briefer (Fig. 2c).

4. Coupling of atmospheric and soil parameters

In this section we explore more closely the links between θ_E and soil temperature; and P_{LCL}, EF, and soil moisture.

a. Relation between θ_E and soil temperature

The daytime solar forcing imposes a strong diurnal cycle of θ_E over land, related to the net daytime energy input and the deepening of the BL. Over the tropical oceans, where the sea surface diurnal cycle is small (except in very light winds), near-surface and BL θ_E are closely related to sea surface temperature. A similar relationship exists in terms of daily means over land. Figure 12a plots daily mean θ_E against daily mean soil temperature for the months Apri1–October for the three years. The scatter in θ_E is considerable (± 8 K), but the increase with mean soil temperature is clear, and it is the same for all three years. Figure 12b shows curves based on averaging the data in 2°C bins of daily mean soil temperature. The heavy solid line is the binned average for all the three years of the data in Fig. 12a for the daily mean θ_E. The heavy dashed curve is a theoretical curve of boundary layer equilibrium θ_E over the oceans from Betts and Ridgway (1989). Despite the added complexity of the diurnal cycle over land, the observed coupling between daily mean θ_E and soil temperature (here at 10 cm) is very close to (but 2–3 K above) this idealized oceanic model. The upper light solid curve is calculated by binning (for all three years) afternoon averages of θ_E (1800–2100 UTC, corresponding roughly to the 3 h after local noon, which is 1820 UTC). This line is about 6 K above the daily mean θ_E line (heavy solid) because of the diurnal range, but has a similar slope. Although we show only the three-year average, all three years are very similar.

The slope $\partial\theta_E/\partial T$ for the oceanic curve on Fig. 12b is quite steep (~3 at 25°C). Over land, at the warmest temperatures, there is some sign of a smaller slope in $\partial\theta_E/\partial T$, probably because these conditions are only reached on days when the soils are dry and evaporation is low, and this has a feedback on θ_E (see section 5). The standard deviation about the day-mean θ_E (the heavy solid line) for each soil temperature class is ± 8 K. Although this is considerable, it is less than the seasonal variation of θ_E, which depends primarily on the variation of soil temperature. The standard deviation of the afternoon mean θ_E values about the thin solid line is a little greater, ± 10 K.

Although the coupling between surface temperature and BL equivalent potential temperature shown on seasonal timescales in Fig. 12 (which is important to the BL control on moist convection) is similar over land and sea, the control on the surface fluxes is quite different, especially on shorter timescales. Over the ocean, the surface temperature strongly influences the surface fluxes, while over land, net radiation is the primary control on the surface fluxes. On seasonal timescales, there is a large storage of energy in the ocean mixed layer so that net radiation and surface fluxes are not coupled on shorter timescales. Over land, the ground storage is a small fraction of the net radiation (Fig. 10), but because the thermal capacity of the first meter of

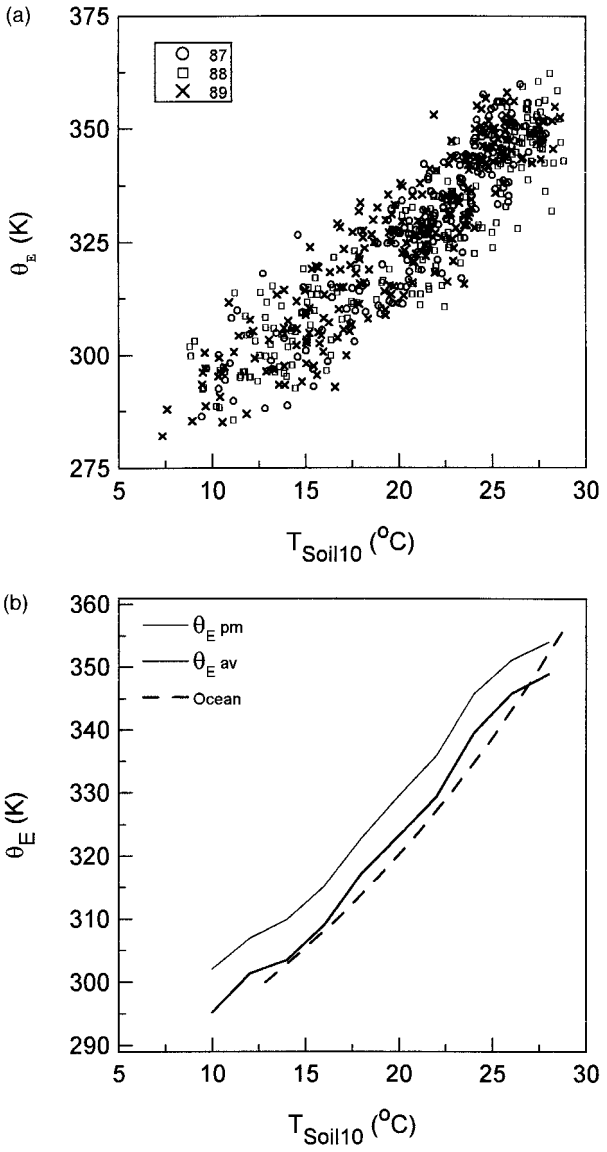

FIG. 12. (a) Scatterplot of daily mean 2-m θ_E against daily mean 10-cm soil temperature for 1987–89. (b) Binned averages of daily mean 2-m θ_E and afternoon mean θ_E (1800–2100 UTC) against 10-cm soil temperature. Heavy dashed line is theoretical line from coupled ocean–atmospheric BL model.

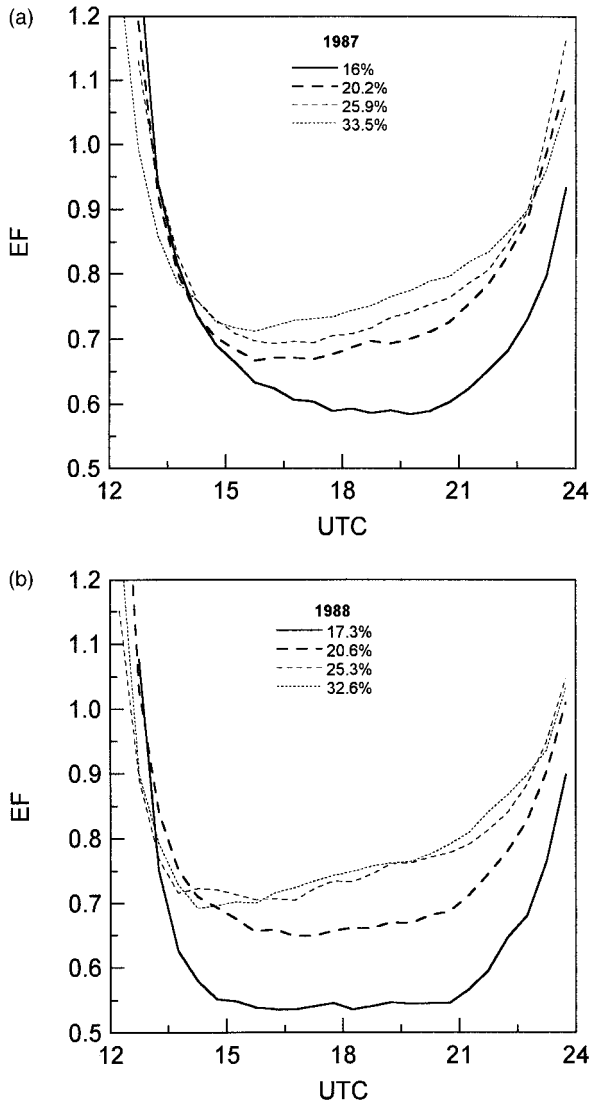

FIG. 13. Diurnal cycle of EF for composites stratified by 0–10-cm soil moisture (a) for 1987 and (b) for 1988.

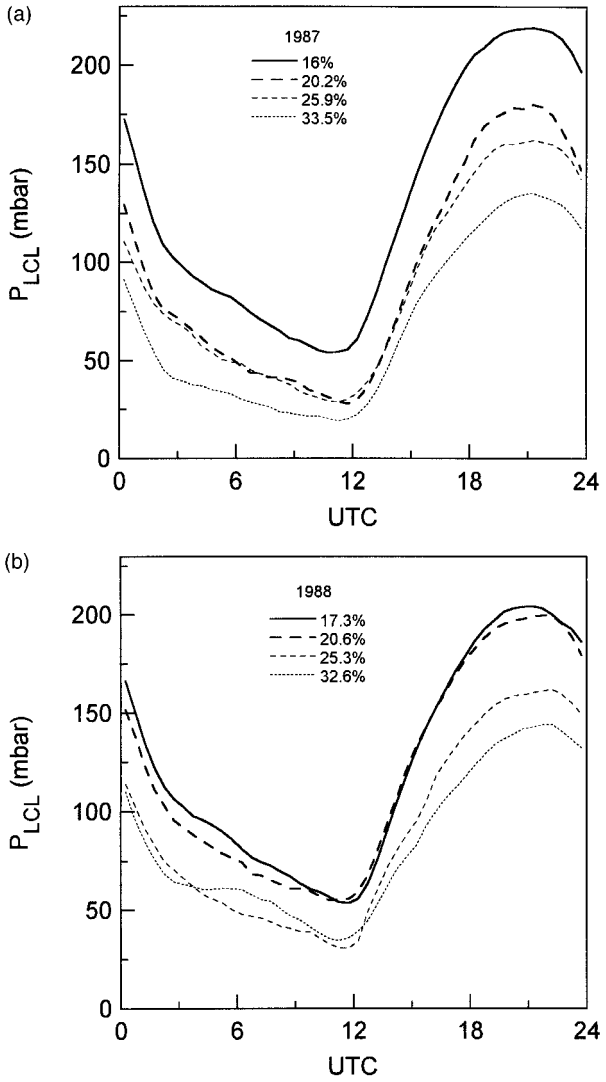

FIG. 14. As in Fig. 13a but for diurnal cycle of P_{LCL} (a) for 1987 and (b) for 1988.

soil is so much less than that of the ocean mixed layer, the seasonal cycle of near-surface temperature can be larger over land than over the ocean (where surface temperatures are also buffered by the lateral transports in ocean currents). This seasonal cycle of soil temperature is both large and important because the daily surface fluxes over land add only increments of θ_E (± 5 K) to this large seasonal trend shown in Fig. 12. We will develop this further in section 5b.

b. Diurnal coupling of soil moisture, EF, and P_{LCL}

We then constructed composites of ''undisturbed'' days based on 0–10-cm soil moisture, selecting days in 4-month periods 30 May–30 Sep 1987 and 20 May–20 Sep 1988, where the soil and weather warmed a little earlier). Our definition of ''undisturbed'' days was days without significant daytime rain and high R_n (above a threshold of 425 W m^{-2} for May, 450 W m^{-2} for June, July, and August, and 400 W m^{-2} for September). We rejected a few days with strong daytime advection of moisture.

Because the 1987 summer was much wetter than 1988, there are rather different numbers of days in each composite since we used the same volumetric soil moisture ranges, summarized in Table 1. Figures 13a and 13b show the diurnal cycle of evaporative fraction, EF, for composites stratified by 0–10-cm soil moisture for 1987 and 1988. The figures are very similar, showing that daytime EF increases as expected with increasing soil moisture. At high soil moistures, the change in EF with soil moisture is small; the vegetation becomes stressed only as soil moisture in this 0–10-cm layer drops below about 20%. Figures 14a,b show the cor-

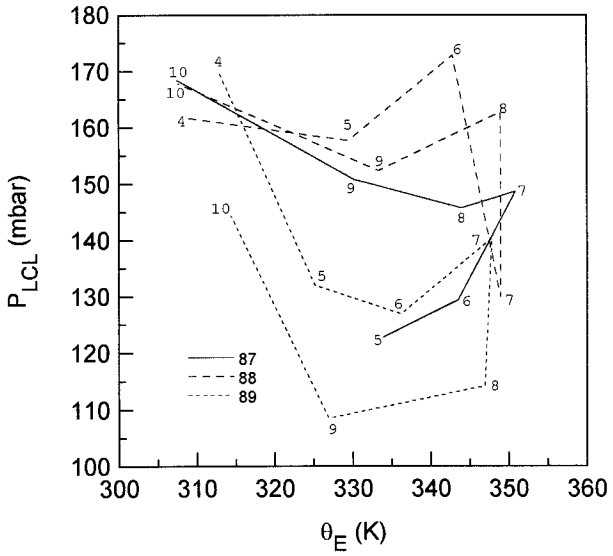

FIG. 15. Seasonal cycle of monthly mean afternoon (1800–2100 UTC) θ_E, P_{LCL}, for 1987–89.

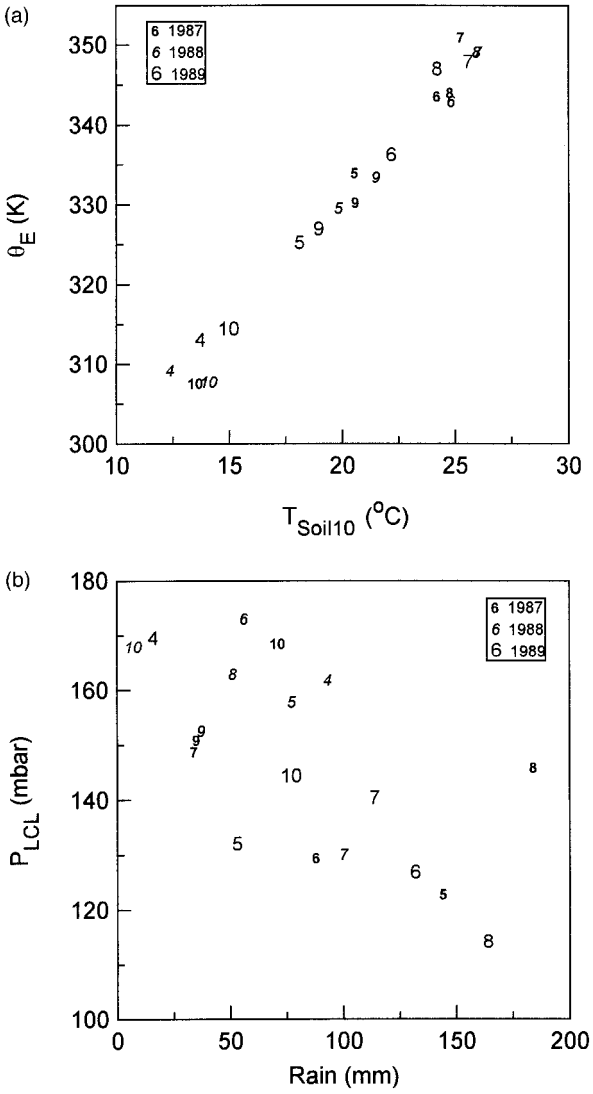

FIG. 16. Monthly mean afternoon (1800–2100 UTC) (a) θ_E versus monthly mean 10-cm soil temperature for 1987–89 (Apr–Oct, excluding Apr 1987) and (b) P_{LCL} versus monthly total rainfall.

responding diurnal graphs of P_{LCL} composited by soil moisture. There are some differences between the years, but the trend toward a higher LCL with drier soils, and lower EF, is clear for both years. Not surprisingly, on average the subsaturation of the air near the surface is linked to the availability of water for evaporation. In contrast over the warm oceans, P_{LCL}, which is typically also cloud base, is around 60 mb. Over land, over the wettest soils, the daily mean P_{LCL} approaches (but remains higher than) this oceanic value.

Table 1 also summarizes some mean parameters for these composites for the 1800–2100 UTC time period, including R_n, G, EF, and P_{LCL}, as well as V_s the mean wind speed and ΔT_{rad}, the difference between the radiometric skin temperature (T_{skin}) and the 2-m air temperature. Values of ΔT_{rad} are generally higher in 1988 than 1987: we do not know if this is a drift of the radiometric skin temperature sensors, or a difference between the years. Also, R_n appears higher in 1988. However, the difference is probably not significant as the calibration of the FLUX R_n sensors in 1987 is still open to question (Smith et al. 1992a). In 1987, they were simply adjusted to a common standard, while for 1988, where only two investigators' data are involved, no adjustment has been made to the data. Our FLUX and PAM R_n averages agree in 1987, while in 1988 the FLUX R_n average is about 15 W m^{-2} higher than the PAM average for these soil moisture stratifications. Note that our site-averaged estimates of G were lower in 1988 than 1987, but this may be because the site locations are different in the two years.

c. Seasonal cycle of afternoon BL equilibrium

Figures 11a–c showed the monthly daytime diurnal cycle of P_{LCL} and θ_E for the three years. If we focus on just the afternoon state (again an 1800–2100 UTC average) and plot the sequence of these for each month, we can compare the seasonal cycle for different years. In Fig. 15, the numbers represent this afternoon state for each month. The first year, 1987 (solid), is perhaps a more normal annual sequence: an anticlockwise progression on this figure. In spring (May = 5) the soils are wet, P_{LCL} is low; and during the summer P_{LCL} rises as the soils dry out (see also Betts and Ball 1995). θ_E rises to a midsummer maximum as the soil warms and then falls. In October 1987, evaporation is low, and P_{LCL} is high. The drought year 1988 has quite a different pattern. It is dry in spring, and P_{LCL} rises to a peak in June, when the *mean* pressure height to the LCL is 45 mb higher than the previous year. July 1988 has significant rainfall (starting, in fact, on 30 June) and P_{LCL}

TABLE 2. Midsummer soil moisture composites.

Year	SM range (%)	$\overline{SM}$ (%)	Number of days	R_n (W m^{-2})	G (W m^{-2})	EF	P_{LCL} (mb)	θ_E (K)	V_s (m s^{-1})	ΔT_{rad} (K)	T_{soil10} (K)
1987	<16	14.7	8	582	100	0.54	239	351.6	5.3	7.0	27.9
	16–23	18.3	10	584	84	0.66	169	354.9	6.0	4.7	26.7
	>23	29.9	10	548	74	0.78	134	360.7	6.1	1.1	26.4
1988	<18.5	17.6	10	560	55	0.60	207	353.1	5.9	6.9	28.7
	18.5–25	21.1	8	563	50	0.74	193	358.3	5.8	4.6	27.6
	>25	28.2	7	581	56	0.82	143	360.8	4.4	4.4	27.5

falls sharply, but returns to a higher level in August. The following year, 1989, again starts dry in spring (April = 4) and has the reverse cycle to 1987, as August and September are much wetter.

Figure 16a, which shows monthly mean afternoon θ_E against daily average soil temperature at 10 cm, depicts a similar relationship to Fig. 12b. Note that the midsummer maximum of θ_E is similar in all years because the soils reach similar temperatures, but in May, June, and September there are significant differences in mean afternoon θ_E, which appear primarily related to mean soil temperature. Figure 16b is a similar plot of afternoon mean P_{LCL} against monthly accumulated rainfall (in mm). Mean afternoon LCL falls with increasing rainfall, but the scatter is larger than in Fig. 16a. Evaporation depends not just on monthly rainfall but on the seasonal cycle of both soil moisture and vegetation. A useful reference number is the midsummer monthly evaporation of about 125 mm mo^{-1}. Only a few months have more precipitation than this. One outlying point is August 1987 when 80 mm of rain fell after a long drought. Another is May 1989, which was a cool month (see Fig. 16a), and perhaps advection is responsible for the relatively low P_{LCL}, as little rain fell locally.

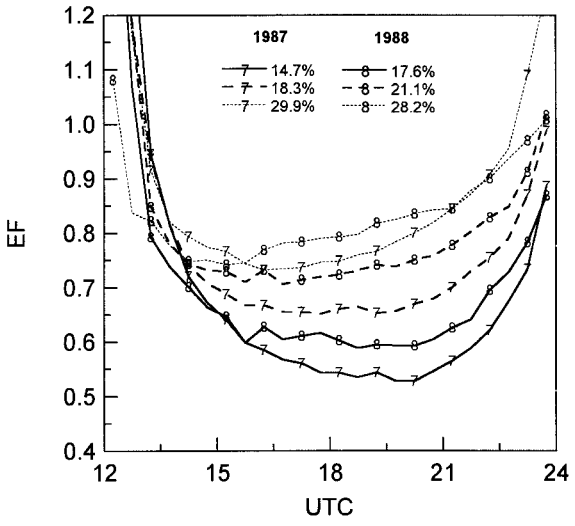

FIG. 17. Evaporative fraction for 1987 and 1988 midsummer soil moisture composites.

5. Local soil moisture–boundary layer feedback

The previous section has illustrated the links between soil moisture and P_{LCL} and soil temperature and θ_E, using data for the whole summer period. Betts and Ball (1995) by stratifying days in midsummer by soil moisture showed that the characteristic diurnal cycle of θ_E for undisturbed days (with the same R_n) was quite different over wet soils than dry soils. Here we will extend this work to include the following summer of 1988. For 1989, soil moisture data is only available for a brief few weeks, giving insufficient days for a composite analysis. We then compare the BL equilibrium state found over warm oceans with this midsummer diurnal cycle over land, which depends on soil moisture.

a. Midsummer coupling of diurnal cycle to soil moisture

For both 1987 and 1988, there is a two-month period in midsummer when 10-cm soil temperatures are around 25°C or greater. This period in 1988 is 10 days earlier (19 June–19 August: Julian days 170–230) than in 1987, when it is during July and August. By choosing periods of similar soil temperature (which has a strong seasonal impact on θ_E: see Figs. 12 and 16a), we can see more clearly the separate impact of soil moisture on the diurnal cycle of both θ_E and P_{LCL}. In the process though, we reduce the number of days in each composite to only 7–10 in each year. For both years we composited the data on the undisturbed days without strong advection during these two-month time periods using 0–10-cm soil moisture. Table 2 summarizes the composites. For 1987 we kept the three soil moisture ranges used in Betts and Ball (1995) (the values are different only because of the error in the gravimetric to volumetric correction in our earlier work). 1987 was a year of greater midsummer extremes. In 1988, we used 3 higher soil moisture ranges, because there were no days with SM < 17%. The tabulated data are, as in Table 1, averages for the time period 1800–2100 UTC. We comment again that the differences in R_n and G between the two years are probably not significant.

Figure 17 shows the expected difference in daytime EF for the six composites for 1987 and 1988, a mirror of Fig. 13 for the soil moisture classes based on the whole summer. Except for the two wettest soil cate-

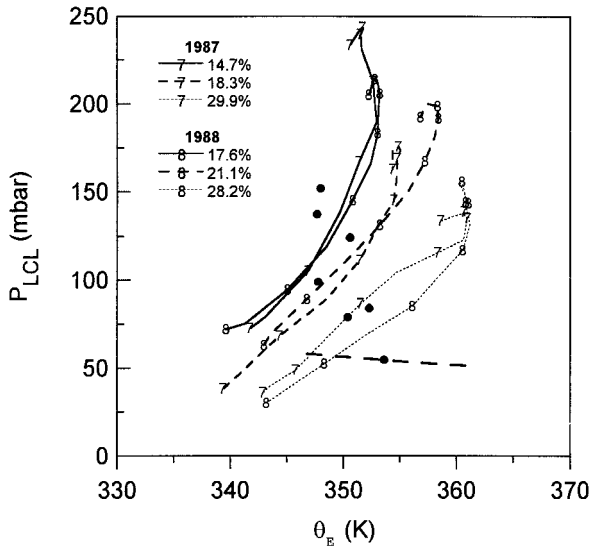

FIG. 18. Daytime diurnal cycle of θ_E, $P_{\rm LCL}$ for 1987 and 1988 midsummer soil moisture composites. The solid circles are daily means, and the heavy dashed line is an oceanic equilibrium line, described in the text.

gories, the progression of curves follows the increase of soil moisture. For these composites the diurnal curves of the R_n are within ± 15 W m^{-2} near local noon (Table 2) so that over dry soils, the surface SH flux is much larger and LH flux significantly less than over wet soils. Figure 18 shows the daytime diurnal cycle for these six composites: the numbers are every two hours from 1115 to 2315 UTC. (The nearly horizontal heavy dashed line and solid circles are discussed in the next section.) We see a general progression for the three composites for both years, although the progression with soil moisture is not completely uniform for all six cases. For the dotted composites with high soil moisture and higher EF, θ_E starts with a higher value at sunrise and rises faster to a higher afternoon maximum near 361 K. In contrast, for the composites with low soil moisture (shown heavy solid), the maximum afternoon θ_E is only about 353 K. Correspondingly $P_{\rm LCL}$, a measure of the height of cloud base, starts higher for the dry soil composites, lifts faster, and reaches a higher afternoon maximum. If we loosely associated $P_{\rm LCL}$ (a measure of cloud base) with the depth of the mixed layer, we can interpret the different daytime θ_E rises in terms of BL depth. The available energy ($R_n - G$) is similar for each composite. This is the surface source of θ_E (Betts and Ball 1995). Over wet soils, θ_E rises more rapidly, both because the BL is less deep and because the slower deepening is associated with less entrainment of low θ_E air at BL top. Note, however, that the difference in afternoon states is only partly associated with the different rates of change during the day. Roughly half the difference is associated with the shift of the dry to wet soil composites toward higher θ_E and lower $P_{\rm LCL}$. This is because after sequential days over wet soils, the BL becomes cooler and moister, closer to saturation, but with a higher θ_E.

The 1988 data confirms the conclusion of Betts and Ball (1995) about the important role of soil moisture on the BL diurnal cycle climate over land. We will restate it as this. Given a similar soil temperature and net available energy (and in the absence of significant horizontal advection), higher soil moisture and the associated higher EF will lead to a higher afternoon equilibrium θ_E and lower cloud base. Since both higher θ_E and lower cloud base favor enhanced deep convention and hence precipitation, here there is an important local positive feedback mechanism between enhanced soil moisture and enhanced precipitation. Since the 12-h daytime diurnal cycle is involved, there is also an implied spatial scale for this thermodynamic surface–BL feedback mechanism, which at 5 m s^{-1} is about 200 km. (There are also the spatial scales of mesoscale convective system dynamics to be considered.) Perturbations of soil moisture on larger spatial scales corresponding to, say, two-day horizontal advection ($\sim$850 km at 5 m s^{-1}) are likely to be even more effective in producing larger BL differences of θ_E and $P_{\rm LCL}$. As noted above, the separation of the dry and wet curves in Fig. 18 is probably caused by the drift of the mean BL state after sequential days over dry or wet soils.

b. *Comparison of equilibria over warm oceans and midsummer diurnal cycle over land*

The nearly horizontal heavy dashed line in Fig. 18 is the equilibrium solution from Betts and Ridgway (1989) for a range of tropical oceanic temperatures from 300 to 303 K and a surface wind speed of 6.7 m s^{-1}. Over the (saturated) ocean, $P_{\rm LCL}$ varies little, whereas θ_E increases rapidly with temperature. The daily average 10-cm soil temperature of our six midsummer composites is 26.6°C, while the afternoon values are given in Table 2. The diurnally averaged total surface sensible and latent heat fluxes are rather similar for the ocean and land cases, although wind speeds and surface roughnesses differ. The solid circle on the dotted ocean curve corresponds to the *same* surface SH + LH = 167 W m^{-2} as the daily average of the six land composites. The other solid circles are the daily average (θ_E, $P_{\rm LCL}$) for the six land composites. Over the ocean, EF = 0.95, while for the land composites the daily mean EF decreases from 0.9 to 0.7 with decreasing soil moisture. The lower EF over land shifts the daily mean equilibrium toward lower θ_E and higher $P_{\rm LCL}$ relative to the ocean equilibrium case. The diurnal forcing over land is superimposed on this daily mean, so that the afternoon state as shown has a still higher $P_{\rm LCL}$, but can over moist soils have a θ_E as high as over the warmest tropical oceans (303 K), thus favoring deep convection. However, as we have noted earlier, over dry soils afternoon $P_{\rm LCL}$ increases further and θ_E increases less, which does not favor deep convection. This range of peak θ_E with

different soil moisture (shown in Fig. 18) corresponds to a 2-K change in sea surface temperature. In the Tropics, the large-scale circulations between continents and oceans depend critically on this θ_E balance at low levels over land and ocean (Eltahir 1996).

6. Conclusions

We have prepared a site-averaged dataset from the FIFE PAM stations from 1 May 1987 to 10 November 1989 (with a 30-min time step), both for the use of single-column model testing and the comparison with gridpoint time series from large-scale models near the FIFE location.

We have also produced FIFE site-averaged surface FLUX datasets (also with a 30-min time step) for the summers of 1987 and 1988 and a three-week period in 1989, as well as corresponding site-averaged soil moisture profiles interpolated to a daily time step. These datasets should be of great value in assessing the performance of land surface models, both interactively in large-scale forecast and climate models and in off-line testing. In this paper we discuss some of the characteristics of the diurnal and seasonal cycles for the three summers, focusing on the physical links between the subsurface variables of soil temperature and moisture, the surface energy budget and surface fluxes, and the 2-m thermodynamic variables, which control the development of the atmospheric BL and atmospheric convection. On the seasonal timescale, the links between precipitation, soil moisture, vegetation, and daytime evaporative fraction are clearly visible. We show that, on seasonal timescales, for undisturbed days soil temperature is coupled to equivalent potential temperature, θ_E; while the pressure of the lifting condensation level (an estimate of the pressure height of cloud base) is linked to soil moisture because this controls evapotranspiration. We draw parallels with the ocean surface boundary condition, where the availability of water is not limiting (and cloud base varies little), but low-level θ_E is also tied closely to the sea surface temperature. Unlike over the ocean, the solar heating over land superimposes a strong diurnal cycle on the mean state, as the surface fluxes are directly forced by the net radiation. We have confirmed using the 1988 FIFE data our conclusion from the 1987 data (Betts and Ball 1995) that in midsummer, when soil temperatures are warm, the effect of soil moisture on the diurnal cycle can be separated by compositing the surface flux and thermodynamic data for undisturbed days as a function of soil moisture. When lack of soil moisture reduces evapotranspiration, the boundary layer becomes deeper and the afternoon state is warmer and drier with a lower θ_E and a higher P_{LCL} as compared to days when soil moisture is plentiful. This, in turn, confirms the possibility of a positive feedback between soil moisture and rainfall on spatial scales comparable to (or larger than) the advection distance over the daytime diurnal cycle (typically 200 km). Precipitation increases soil moisture, which gives a lower afternoon cloud base and higher θ_E, which in turn favors more precipitating convection in a region.

We also discuss the diurnal and seasonal variation of albedo for this site. Seasonally the main difference is transitory snowfall in winter, which for this Kansas site increases the albedo to 0.6–0.8, typically for a few days with each snow event. We comment that it may be important to include the diurnal rise of albedo near sunrise and sunset into models, which predict a surface radiative equilibrium temperature. We show, from the 1988 season, the reduction of the soil heat flux at night with drier soils, suggesting further feedbacks between soil moisture and the surface energy budget that may need to be included in models for grasslands.

In conclusion, FIFE collected a rich dataset for studies of the land surface–atmosphere interaction for the midcontinental grassland ecosystem, which will be invaluable for years to come.

Acknowledgments. This research has been supported by NASA under Contract NAS5-32356, and NSF under Grant ATM95-05018. We acknowledge the dedication of all those who collected, processed, and archived the FIFE datasets, and we particularly acknowledge the scientific leadership of Piers Sellers. We are grateful to Leo Fritschen and Dalin Nie, who recovered some of the 1988 FLUX datasets. It is appropriate ten years after the first field phase of FIFE to acknowledge the foresight of the NASA Ecosystems Dynamics Branch under Dianne Wickland, for her long-term support of a broad program, which extends all the way from a surface ecosystem study to providing key understanding of the land-surface boundary conditions for global models.

APPENDIX

FIFE Site-Mean Datasets

a. PAM data

Time period 1 May 1987–10 November 1989
Frequency: 30 min

Variable list

Date	
Time	(UTC)
p	Pressure (mb)
T	2-m air temperature (°C)
T_w	2-m wet-bulb temperature (°C)
q	2-m mixing ratio (g kg^{-1})
u	2-m west–east wind component (m s^{-1})
v	2-m south–north wind component (m s^{-1})
T_{surf}	Radiometric surface temperature (°C)
$T_{\mathrm{soil}\,10}$	10-cm soil temperature (°C)
$T_{\mathrm{soil}\,50}$	50-cm soil temperature (°C)

$S\downarrow$	Incoming solar radiation (W m^{-2})
$S\uparrow$	Reflected solar radiation (W m^{-2})
R_n	Net radiation (W m^{-2})
$L\downarrow$	Incoming longwave radiation (W m^{-2})
Rainfall	From tipping bucket (mm)

Comments. The wet bulb freezes, so q is unreliable for $T_w < 0$°C. The radiation instruments were all removed for calibration, 11 April–10 May 1988. Calibration differences between the PAM and FLUX radiation instruments are not reconciled here. We did not process the data for photosynthetically active radiation.

b. FLUX data

Time periods: 27 May 1987–16 October 1987
10 May 1988–19 September 1988
21 July 1989–14 August 1989
Time frequency: 30 min

Variable list

Date	
Time	(UTC)
R_n	Net radiation (W m^{-2})
G	Ground heat flux (W m^{-2})
LH	Latent heat flux (W m^{-2})
SH	Sensible heat flux (W m^{-2})
$S\downarrow$	Incoming solar flux (W m^{-2})
$S\uparrow$	Reflected solar flux (W m^{-2})
$L\downarrow$	Incoming LW flux (an average of two stations in 1987 and one in 1989)
$L\uparrow$	Outgoing LW flux (an average of two stations in 1987 and one in 1989)

Where available, these radiation data are probably superior to the PAM data either because of better instrument calibration (e.g., LW$\downarrow$) or better sampling ($S\downarrow$ in 1988 summer). However, issues of R_n calibration were not resolved in the 1987 datasets (Smith et al. 1992a).

c. Soil moisture data

Gravimetric data

Levels 0–5 cm
5–10 cm

Time periods: 20 May 1987–6 November 1987
11 April 1988–21 October 1988
19 July 1989–12 August 1989

Time frequency: variable, from daily to as long as weeks.

Data has been interpolated on a site basis to daily values before averaging. In this paper we have converted the gravimetric values to volumetric values using a bulk density of 1.1:

$$\mathrm{SM}_v = 1.1\ \mathrm{SM}_g.$$

The subscript v is omitted in the text.

Neutron probe data 20–200 cm.

Levels: 20, 30, 40, 50, 60, 80, 100, 120, 140, 160, 180, 200 cm, merged with 0–10 cm gravimetric data at each site converted to volumetric value. Tubes were inserted at each site as deeply as possible. Median soil depth was 1.5 m (Duan et al. 1995).

TABLE A1. Nominal mean soil properties for FIFE site [data from John Norman (1996, personal communication)].

Layer (cm)	Bulk density (kg m^{-3})	Sand (%)	Silt (%)	Clay (%)
0–15	1.1	0.10	0.55	0.35
15–40	1.3	0.05	0.40	0.55
40–100	1.4	0.15	0.45	0.40

Time periods: 29 May 1987–6 November 1987
11 April 1988–29 September 1988
24 July 1989–8 August 1989

Time frequency: The sampling frequency of the neutron probe data is generally less than that of the near-surface gravimetric data: typically every few days in 1987 and 1989 (for only three weeks) and every week in 1988. See Table A1 for soil property distribution.

Comments. There are some apparent inconsistencies between the 1987 and 1988 neutron probe data that we cannot reconcile from the published documentation. The highest neutron probe level (at 20 cm) in 1987 is clearly unreasonable (values are often drier than at levels above and below). This is not unexpected since the effective range of this neutron device, particularly in dry soils, exceeds 20 cm. This instrumental limitation means that we have no reliable data in the important depth range 10–30 cm. In contrast, in 1988, the published 20-cm data fits a uniform progression with depth. We suspect a change in reference depth procedures. While the soil moisture data appears qualitatively correct, and extremely useful, the change of vertically integrated soil moisture (calculated from the neutron probe dataset), in Fig. 1, is less than the precipitation − evaporation difference by 40 mm in the summer of 1987 and 110 mm in the summer of 1988. Although precipitation is likely to be underestimated, and evaporation could be overestimated, we recommend caution in using the neutron probe soil moisture data as quantitative truth for long-term integrations.

Note that the volumetric soil moisture values in Figs. 17 and 18 are larger than those in Betts and Ball (1995) for the corresponding 1987 composites because in our earlier work (and Betts et al. 1993) we made an error in interpreting the FIFE ''bulk soil density'' measurements (which were described in places as wet soil densities, when they are actually the ratio of the mass of the dried soil sample to its original wet volume before drying). In the earlier papers we converted gravimetric soil moisture (SM_g) to a volumetric value (SM_v) using the incorrect formula $\mathrm{SM}_{V\mathrm{old}} = 1.1\ \mathrm{SM}_g/(1 + \mathrm{SM}_g)$ when in fact ($\mathrm{SM}_v = 1.1\ \mathrm{SM}_g$) is correct for the FIFE bulk soil density of 1.1. The volumetric soil moisture

values (SM_{Vold}) in Betts and Ball (1995) should all be scaled upward using the correction formula:

$$SM_v = 1.1\ SM_{Vold}/(1.1 - SM_{Vold}).$$

For $SM_{Vold} = 0.2$, the correction factor is 1.22.

REFERENCES

Betts, A. K., 1992: FIFE atmospheric boundary layer budget methods. *J. Geophys. Res.*, **97,** 18 523–18 532.

——, 1994: Relation between equilibrium evaporation and the saturation pressure budget. *Bound.-Layer Meteor.*, **71,** 235–245.

——, and W. L. Ridgway, 1989: Climatic equilibrium of the atmospheric convective boundary layer over a tropical ocean. *J. Atmos. Sci.*, **46,** 2621–2641.

——, and J. H. Ball, 1994: Budget analysis of FIFE-1987 sonde data. *J. Geophys. Res.*, **99,** 3655–3666.

——, and ——, 1995: The FIFE surface diurnal cycle climate. *J. Geophys. Res.*, **100,** 25 679–25 693.

——, and A. G. Barr, 1996: FIFE 1987 sonde budget revisited. *J. Geophys. Res.*, **101,** 23 285–23 288.

——, R. L. Desjardins, and J. I. MacPherson, 1992: Budget analysis of the boundary layer grid flights during FIFE-1987. *J. Geophys. Res.*, **97,** 18 533–18 546.

——, J. H. Ball, and A. C. M. Beljaars, 1993: Comparison between the land surface response of the European Centre model and the FIFE-1987 data. *Quart. J. Roy. Meteor. Soc.*, **119,** 975–1001.

——, ——, A. C. M. Beljaars, M. J. Miller, and P. Viterbo, 1996a: The land–surface–atmosphere interaction: A review based on observational and global modeling perspectives. *J. Geophys. Res.*, **101,** 7251–7268.

——, S.-Y. Hong, and H.-L. Pan, 1996b: Comparison of NCEP/NCAR Reanalysis with 1987 FIFE data. *Mon. Wea. Rev.*, **124,** 1480–1498.

——, F. Chen, K. Mitchell, and Z. Janjić, 1997: Assessment of land surface and boundary layer models in two operational versions of the Eta Model using FIFE data. *Mon. Wea. Rev.*, **125,** 2896–2916.

Chen, F., K. Mitchell, J. Schaake, Y. Xue, H.-L. Pan, V. Koren, Q. Duan, and A. Betts, 1996: Modeling of land–surface evaporation by four schemes and comparison with FIFE observations. *J. Geophys. Res.*, **101,** 7251–7268.

Desjardins, R. L., P. H. Schuepp, J. I. MacPherson, and D. J. Buckley, 1992: Spatial and temporal variations of the fluxes of carbon dioxide and sensible and latent heat over the FIFE site. *J. Geophys. Res.*, **97,** 18 467–18 476.

Duan, Q. Y., J. C. Schaake, and V. I. Koren, 1996: FIFE 1987 water budget analysis. *J. Geophys. Res.*, **101,** 7197–7207.

Eltahir, E. A. B., 1996: Role of vegetation in sustaining the large-scale atmospheric circulations in the Tropics. *J. Geophys. Res.*, **101,** 4255–4268.

Famiglietti, J. S., E. F. Wood, M. Sivapalan, and D. J. Thongs, 1992: A catchment scale water balance model for FIFE. *J. Geophys. Res.*, **97,** 18 997–19 007.

Fritschen, L. J., and P. Qian, 1992: Variation in energy balance components from six sites in a native prairie three years. *J. Geophys. Res.*, **97,** 18 651–18 662.

——, ——, E. T. Kanemasu, D. Nie, E. A. Smith, J. B. Stewart, S. B. Verma, and M. L. Wesely, 1992: Comparisons of surface flux measurement systems used in FIFE 1989. *J. Geophys. Res.*, **97,** 18 697–18 714.

Grossman, R. L., 1992: Convective boundary layer budgets of moisture and sensible heat over an unstressed prairie. *J. Geophys. Res.*, **97,** 18 425–18 438.

Hall, F. G., K. F. Huemmrich, S. J. Goetz, P. J. Sellers, and J. E. Nickerson, 1994: Satellite remote sensing of surface energy balance: Success, failures, and unresolved issues in FIFE. *J. Geophys. Res.*, **97,** 19 061–19 090.

Kanemasu, E. T., S. B. Verma, E. A. Smith, L. J. Fritschen, M. Wesely, R. T. Field, W. P. Kustas, H. Weaver, J. B. Stewart, R. Gurney, G. Panin, and J. B. Moncrieff, 1992: Surface flux measurements in FIFE: An overview. *J. Geophys. Res.*, **97,** 18 547–18 556.

Kelly, R. D., 1992: Atmospheric boundary layer studies in FIFE: Challenges and advances. *J. Geophys. Res.*, **97,** 18 373–18 376.

Nie, D., T. Demetriades-Shah, and E. T. Kanemasu, 1992: Surface energy fluxes on four slope sites during FIFE 1988. *J. Geophys. Res.*, **97,** 18 641–18 650.

Sellers, P. J., F. G. Hall, G. Asrar, D. E. Strebel, and R. E., Murphy, 1992: An overview of the First International Satellite Land Surface Climatology Project (ISLSCP) Field Experiment (FIFE). *J. Geophys. Res.*, **97,** 18 345–18 371.

Smith, E. A., W. L. Crosson, and B. D. Tanner, 1992a: Estimation of surface heat and moisture fluxes over a prairie grassland. Part 1: In situ energy budget measurements incorporating a cooled mirror dew point hygrometer. *J. Geophys. Res.*, **97,** 18 557–18 582.

——, A. Y. Hsu, W. L. Crosson, R. T. Field, L. J. Fritschen, R. J. Gurney, E. T. Kanemasu, W. P. Kustas, D. Nie, W. J. Shuttleworth, J. B. Stewart, S. B. Verma, H. L. Weaver, and M. L. Wesely, 1992b: Area-averaged surface fluxes and their time–space variability over the FIFE experimental domain. *J. Geophys. Res.*, **97,** 18 599–18 622.

——, M. M.-K. Wai, H. J. Cooper, M. T. Rubes, and A. Hsu, 1994: Linking boundary layer circulations and surface processes during FIFE 89. Part I: Observational analysis. *J. Atmos. Sci.*, **51,** 1497–1529.

Stewart, J. B., and S. B. Verma, 1992: Comparison of surface fluxes and conductances at two contrasting sites within the FIFE area. *J. Geophys. Res.*, **97**, 18 623–18 628.

Verma, S. B., J. Kim, and R. J. Clement, 1992: Momentum, water vapor and carbon dioxide exchange at a centrally located prairie site. *J. Geophys. Res.*, **97**, 18 629–18 639.

Viterbo, P., and A. C. M. Beljaars, 1995. An improved land–surface parameterization in the ECMWF model and its validation. *J. Climate*, **8,** 2716–2748.